PERFORMING SPATIAL ANALYSIS ON TROPICAL CYCLONE RAINBAND STRUCTURES AFTER CREATING A 3D MOSAIC OF WSR-88D REFLECTIVITY DATA USING A MAP-REDUCE FRAMEWORK AND A GEOGRAPHIC INFORMATION SYSTEM (GIS)

Corene J. Matyas *, Jingyin Tang, Stephanie E. Zick
University of Florida, Gainesville, Florida

1. INTRODUCTION

Modeling of tropical cyclones (TCs) allows a better understanding of processes leading to heavy rainfall and inland flooding. High-resolution numerical weather prediction models are utilized operationally to predict TC position, intensity, and rainfall, and are used in research studies to improve understanding of processes contributing to high rain rates and other storm characteristics. The high spatial and temporal resolution data produced by ground-based radars provide important observations of storm structure over land. To facilitate the spatial analysis of radar observations, we develop a Map-reduce-based playback framework to interpolate large volumes of radar data onto 3D grids. We utilize a Geographic Information System (GIS) to interpolate values at grid points and calculate shape metrics to quantify the spatial distribution of reflectivity values at constant altitudes. These shape metrics allow us to numerically relate observed data from the Weather Surveillance Radar 1988 Doppler (WSR-88D) network to modeled storms.

Hurricane Isabel (2003) made landfall as a Category 2 storm at Drum Inlet, NC, on September 18 at 1700 UTC (Lawrence et al. 2005). We select Isabel for analysis due to its large size and good predictions of track and extent of rainfall (NOAA 2003). As forecast models handled the system well, we hypothesize that a model simulation should be able to accurately reproduce the intensity and spatial arrangement of rainbands. To test this hypothesis, we quantify the size, position, and spatial attributes of Isabel's rainfall regions for simulations of reflectivity from the Weather Research and Forecasting (WRF) model and Level II radar data from the WSR-88D network that we mosaic to a 3D grid.

* *Corresponding author address:* Corene J. Matyas, Univ. of Florida, Dept. of Geography, Gainesville, FL 32611-7315; e-mail matyas@ufl.edu

2. WSR-88D REFLECTIVITY PROCESSING

We employ a map-reduce framework (Lakshmanan and Humphrey 2014) to process Level II reflectivity data from radars within 600 km of the storm center (Fig. 1). We construct our system using the concept of an actor model (Byrd et al. 1982), and implement it with Apache Spark and ArcGIS Runtime using Scala programming language. All inputs, intermediate results and outputs are represented as key-values pairs. This allows us to chain multiple map and reduce functions in a pipeline to operate on complex tasks in map-reduce jobs. The complete procedure includes four steps: preprocess, map function chain, reducing function chain and post-process.

After quality control and pre-processing, data are gridded at 250 m x 250 m x 250 m resolution every 5 minutes using data from a 10-minute moving window. Values for grid cells with data from multiple radars are calculated using a time-distance weighted function (Lakshmanan et al. 2006). Cells with missing values are filled using a distance-weighted interpolation performed in a Geographic Information System (GIS). We then draw contours every 5 dB*Z*, execute a smoothing algorithm, and convert the contours into polygons.

We employ ArcGIS runtime to integrate with the system for three main reasons: (1) Geospatial analytics function, namely "geoprocessing," in ArcGIS software is considered to be robust (Steiniger and Bocher 2009). (2) ArcGIS runtime contains a lightware core which can be deployed easily on multiple nodes without a complicated configuration and heavy dependencies on Graphics User Interface libraries. (3) ArcGIS runtime provides a Java-based SDK capable of collaborating with Scala and Apache Spark. Our method also allows users to replace the ArcGIS part with similar implementations as long as these functions are able to accept and return key-pair RDDs.

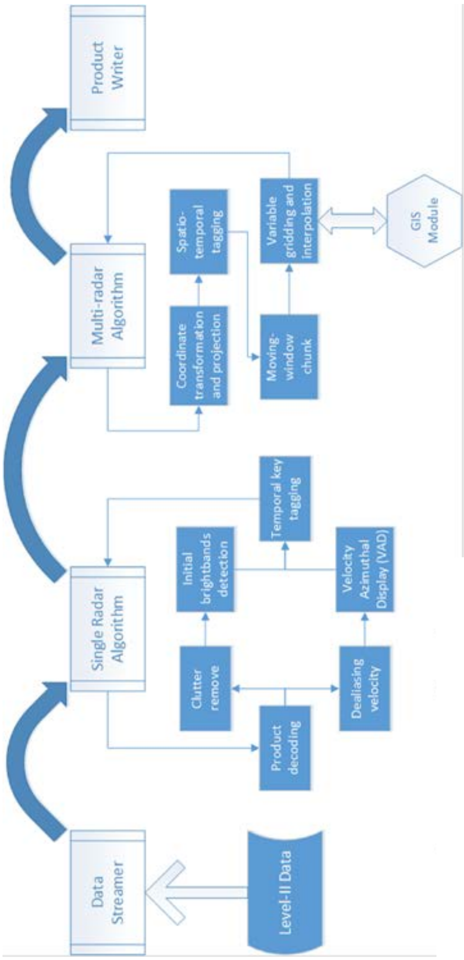

Fig. 1. Radar processing flowchart.

3. WRF MODEL SETUP

This study uses the Advanced Research Weather Research and Forecasting (WRF-ARW) model version 3.4.1 (Wang et al. 2012). The WRF model solves the fully compressible, non-hydrostatic Euler equations using a mass-based terrain-following vertical coordinate (Skamarock et al. 2008). The model domain is triply nested through two-way nesting with a course domain of 27 km horizontal resolution and two inner nests of 9 and 3 km resolution, respectively (Fig. 2). All nests include 40 vertical levels and a model top of 2 hPa, unless otherwise noted. The operational National Centers for Environmental Prediction (NCEP) Global Forecast System (GFS) final analysis is used for the initial and boundary conditions of the simulation. The coarse domain is initialized at 00 UTC September 16, and the inner nests are initialized 24 hours later at 00 UTC September 17. According to best track data, Hurricane Isabel makes landfall at 17 UTC September 18. All simulations are integrated through 00 UTC September 20 to fully encompass the landfall period.

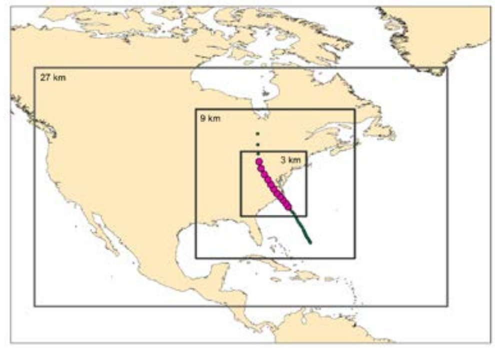

Fig. 2 WRF domain configuration and best track data for Isabel (2003). Large circles represent positions modeled during our simulations.

Before analysis of the simulated storm structure commences, it is necessary to first select an appropriate set of model physics packages. WRF is a highly modular modeling system, with the user specifying not only the domain and time configuration but also the physical parameterizations. Modeling of tropical cyclones is known to be highly sensitive to physical processes (e.g., Davis and Bosart 2002; Wang 2002). In addition, simulated reflectivity depends on the model's microphysics scheme (Koch et al. 2005; Stoelinga 2005). Thus, this research will consider an ensemble of simulations with varying microphysics. However, prior to the development of a 3-km ensemble, we first conduct a series of coarse grid simulations with three different cumulus physics options (Table 1) since the cumulus parameterization of the outermost grids has been shown to impact the convection resolved on the innermost grid (Warner and Hsu 2000). Two of these model configurations are intended to approximately follow the operational physics packages employed in the NCAR WRF-ARW real-time hurricane (WRF-NCARRT) and NCEP Hurricane WRF (WRFSAS) models. The Kain Fritsch cumulus scheme is also selected since it has demonstrated adequate performance in numerous previous research studies (e.g., Davis et al. 2008; Gentry and Lackmann 2010). One additional simulation (Table 1) is conducted with

50 vertical levels, which should better represent the HWRF's higher vertical resolution, although a true HWRF comparison cannot be made with the WRF-ARW dynamic core.

Table 1. Coarse domain set-up for simulations of Hurricane Isabel.

	Cumulus physics	**# vertical levels**
WRF-NCARRT	Tiedtke	40
WRF-SAS	Simplified Arakawa Schubert	40
WRF-KF	Kain-Fritsch	40
WRF50v	Simplified Arakawa Schubert	50

Model storm intensities for these four simulations versus best track are displayed in Fig. 3 a,b. Initialization times of +/- 6 hours were also investigated (not shown) with the best intensity evolution obtained when the coarse grid was initialized at 00 UTC September 16. The WRF50v simulation becomes the most intense, but near the end of the simulation, it becomes unstable. Intensities in the remaining three simulations are comparable, with the WRF-NCARRT simulated storm reaching slightly stronger intensities, based on both the minimum mean sea level pressure ($MSLP_{min}$) and maximum sustained 10-meter wind speeds. Furthermore, there is a better timing of landfall (Fig. 3 c,d) and better representations of WRF forecast accumulated precipitation compared with radar reflectivities as the simulated storms approach and make landfall (Fig. 4) in the WRF-NCARRT simulation. The Kain Fritsch simulation (Fig. 4h) shows completely eroded eyewall to the east of the circulation center, but otherwise displays promising results in its representation of outer convective bands and should be further investigated in future work.

Based on these coarse grid simulated storms, we selected the WRF-NCARRT set-up as optimal for further investigation into a higher-resolution simulation of Hurricane Isabel. For all future analyses, we present results from a simulation with the following physics packages: WRF Single-Moment 6-class microphysics and Yonsei University (YSU) boundary layer scheme. The Tiedtke convective parameterization is utilized for 27 and 9 km simulations but turned off for the 3 km simulation.

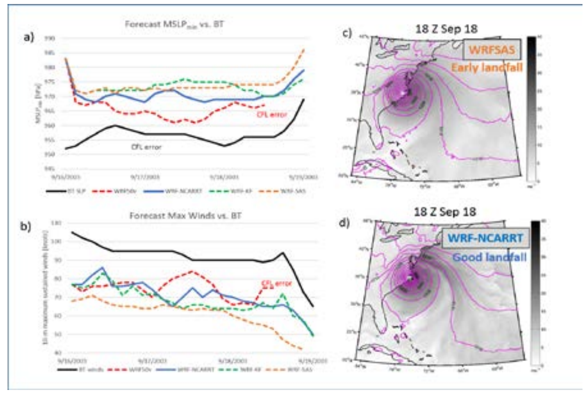

Fig. 3 Comparisons of model and best track a) minimum sea level pressure and b) maximum sustained winds. Isobars at landfall for c) WRFSAS and d) WRF-NCARRT.

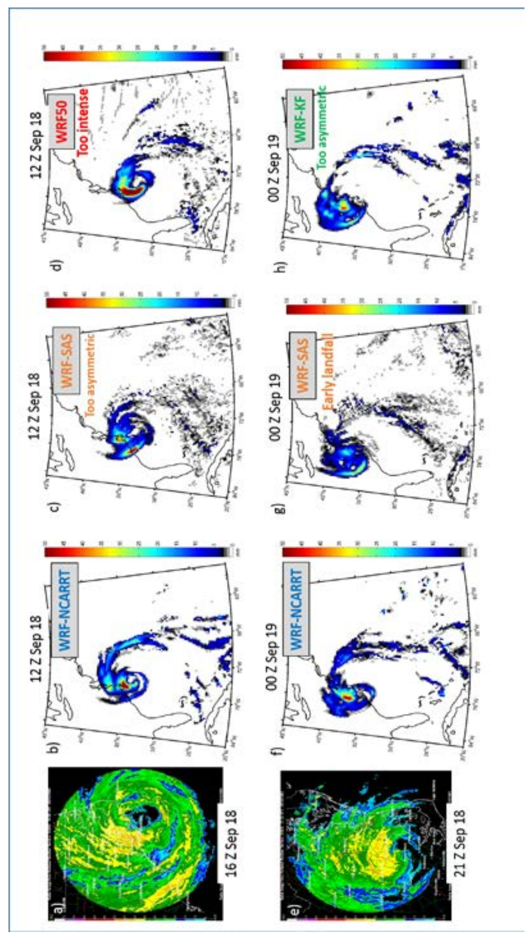

Fig. 4. Observed radar reflectivity values a) and e) and comparisons to simulated reflectivity values at times before and after landfall.

4. **SHAPE METRIC CALCULATIONS**

We next quantify the spatial arrangement of polygons bounded by reflectivity values 20-45 dB*Z* every 5 dB*Z* (Fig. 5). The distance and bearing of polygon centroids are calculated relative to the storm center and used to measure fragmentation and dispersion (A) (Zick and Matyas 2014). Area is combined with perimeter to calculate compactness (B) (MacEachren 1985). The ratio of width to length permits calculation of elongation (C) (Maddox 1980) and orientation (Williams and Wentz 2008). Perimeter length is also used for convexity (D), which is the ratio between perimeters of the shape and its convex hull (Jamil et al. 1993). Determining the convex hull permits the calculation of solidity (E), which compares the shape's area to the area of its convex hull (Jiao et al. 2012). As TC rainbands tend to curve, we quantify the degree of closure around a circle for polygons that do not fully encircle the storm center (F) (Matyas and Tang 2015). We also calculate the percent of intersection between polygons produced by the WRF simulation and those from the radar observations. These measures help determine differences in rainfall regions and identify the best match of model to observations. Though all 40 or 45 dBZ areas are shown in Fig. 5, we only compare the largest polygons with areas >200 sq. km.

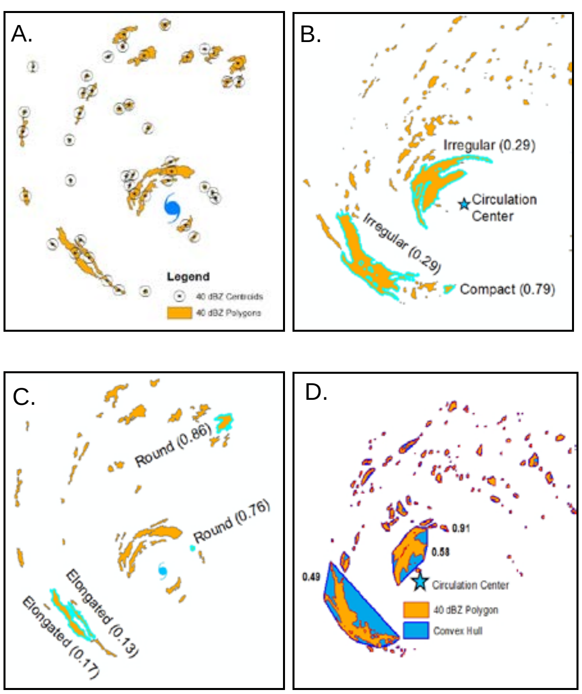

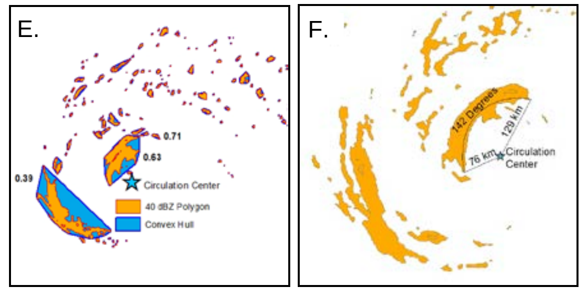

Fig. 5. Position and shape metrics identified in the paragraph above.

4. RESULTS AND DISCUSSION

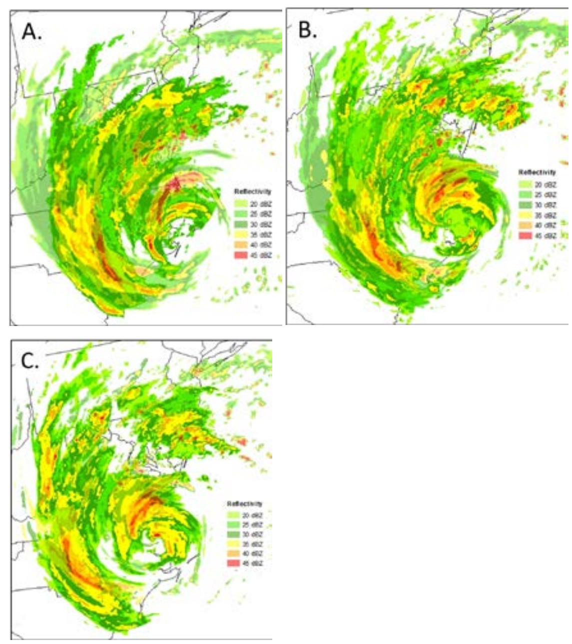

Fig. 6. 3.5 km reflectivity at A) 1700, B) 1830, C) 2000 UTC. WRF values are transparent.

Although landfall occurred ~1 hour earlier and 120 km north in WRF, the high reflectivity polygons southwest of the center have similar position and shape (Fig. 6a). At 1830 UTC, high reflectivity polygons surrounding the core are similar in shape and orientation despite the WRF centroid's offset of 60 km northwest (Fig. 6b). Yet, the model fails to produce the high reflectivity values over Maryland, which explains the increase in the number of radar-observed 40 dB*Z* polygons (Table 1). By 2000 UTC (Fig. 6c), WRF does not depict the broadening of the 35 dB*Z* region in the storm's core, a feature on radar also noted after Hurricane Charley's (2004) landfall (Matyas 2009). The model also moves the storm too quickly inland and exposes its core to environmental air more rapidly than was observed by radar (Table 1, column F), indicating an accelerated extratropical transition process (Gautam et al. 2008). Overall, the polygons with area greater than 200 km^2 are consistent in number across the three WRF outputs, but they are smaller in area than the radar polygons.

Due to model parameterization and resolution, we expected the WRF shapes to have less complex perimeters, yielding lower length values. Mann-Whitney *U* tests confirmed that compactness and convexity were significantly different between radar and WRF at each time. We did retain the null hypothesis of shape similarity for elongation, solidity, and orientation. Table 1 illustrates the similarity in elongation (C) and solidity (E), while the WRF shapes are more compact (B) with perimeters having similar lengths relative to their convex hull (D). Despite the differences in perimeter, the position and orientation of the larger polygons match fairly well between the observed and simulated reflectivity values, particularly on the southwestern edge of the circulation.

Table 1. Median values for 40 dB*Z* (radar) and 45 dB*Z* polygons (WRF) with area >200 sq. km. Letters B-F correspond to Figure 2. Closure is for the storm core.

	n	B	C	D	E	F
Radar 1700	15	0.48	0.33	0.72	0.66	210°
WRF 1700	9	0.53	0.36	0.89	0.67	170°
Radar 1830	20	0.50	0.36	0.79	0.67	200°
WRF 1830	11	0.70	0.38	0.93	0.78	160°
Radar 2000	16	0.47	0.35	0.75	0.61	180°
WRF 2000	10	0.67	0.48	0.89	0.76	80°

Mann-Whitney *U* tests compared the shape metrics of the radar-observed 40 dB*Z* regions to the WRF 40 and 45 dB*Z* regions. Results show that the shapes of the 45 dB*Z* simulated regions were more similar to those of the observed 40 dB*Z* polygons, confirming that the WRF produced reflectivity values that were too high. Given the differences in area among the two datasets, we estimate that the WRF reflectivity values were approximately 4 dB*Z* too high. Although the "best" WRF simulation produced slower wind speeds compared to the best track as the storm approached land and during landfall, its minimum central pressure correlated highly with that of the best track (Fig. 4), indicating a good representation of intensity. While we conclude that the WRF simulated reflectivity values accurately depicted shape and orientation, we hypothesize that the high reflectivity values may stem from the simplifying assumptions of a single-moment bulk microphysics scheme (Lang et al. 2011) and/or a high bias that is frequently observed in WRF simulations (e.g., Done et al. 2004, Davis et al. 2008).

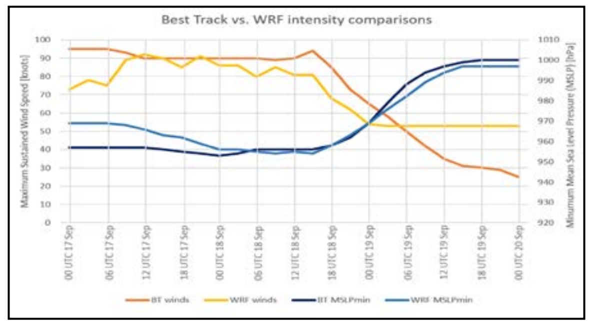

Fig. 4. Comparison of WRF minimum mean sea level pressure and maximum sustained wind speeds to the Best Track (BT). Time begins at inner nest initialization.

5. CONCLUSIONS AND FUTURE WORK

Many previous studies in meteorology rely on visual comparisons to assess the accuracy of model output. Our study calculated shape metrics to compare reflectivity values present in a simulation of Hurricane Isabel (2003) to those observed by WSR-88D units during Isabel's landfall. The shape metrics showed that despite differences in perimeter length due to the more coarse resolution of the WRF values, the position and orientation of polygons representing higher rain rates within Isabel matched fairly well. Thus, we conclude that the calculation of shape metrics facilitates numerical comparisons of observed and modeled radar data.

Building on the previous work of Matyas (2007, 2010), our future work aims to calculate shape metrics on the radar reflectivity values for a larger sample of U.S. landfalling tropical cyclones to permit intra and inter-storm comparisons of rainband shapes, positions, and sizes. We will improve upon the map-reduce framework for the mosaicking of radar data to facilitate rapid yet accurate processing of large volumes of radar data since 1995 (Tang and Matyas, 2015).

On the modeling side, our future work will investigate more complex microphysical parameterizations to better account for hydrometeor distributions. To make the perimeters of the polygons more similar, we will regrid the WSR-88D reflectivity data to a 3 km resolution to match WRF and recalculate our shape metrics. Although this may eliminate many of the small regions of high reflectivity, it should simplify the perimeters of the 20-40 dBZ polygons and bring the AP ratio and convexity measures closer together when comparing the two datasets.

6. REFERENCES

Byrd, R.J., S.E. Smith, and S. P. deJong, 1982: An actor-based programming system. Vol. 3. No. 1-2. ACM.

Davis, C., and L. F. Bosart, 2002: Numerical simulations of the genesis of Hurricane Diana (1984). Part II: Sensitivity of track and intensity prediction. *Mon. Weather Rev.*, **130**, 1100–1124.

——, and Coauthors, 2008: Prediction of landfalling hurricanes with the advanced hurricane WRF model. *Mon. Weather Rev.*, **136**, 1990–2005, doi:10.1175/2007MWR2085.1.

Done, J., C. Davis, and M. Weisman, 2004: The next generation of NWP: Explicit forecasts of convection using the Weather Research and Forecast (WRF) Model. *Atmos. Sci. Lett.*, **5,** 110–117. doi: 10.1002/asl.72

Gautam, R., G. Cervone, R. P. Singh, and M. Kafatos, 2005: Characteristics of meteorological parameters associated with Hurricane Isabel. *Geophysical Research Letters*, **32,** Art. No. L04801.

Gentry, M. S., and G. M. Lackmann, 2010: Sensitivity of Simulated Tropical Cyclone Structure and Intensity to Horizontal Resolution. *Mon. Weather Rev.*, **138**, 688–704, doi:10.1175/2009mwr2976.1.

Jamil, N., Z. A. Bakar, and T. M. T. Sembok, 1993: Image retrieval of songket motifs using simple shape descriptors. *Geometric Modeling and Imaging--New Trends, 2006*, IEEE, 171-176.

Jiao, L., Y. Liu, and H. Li, 2012: Characterizing land-use classes in remote sensing imagery by shape metrics. *ISPRS Journal of Photogrammetry and Remote Sensing*, **72,** 46-55.

Koch, S. E., B. Ferrier, M. T. Stoelinga, E. Szoke, S. J. Weiss, and J. S. Kain, 2005: The use of simulated radar reflectivity fields in the diagnosis of mesoscale phenomena from high-resolution WRF model forecasts. 11th Conf. on Mesoscale Processes, Albuquerque, NM.

Lakshmanan, V., and T. W. Humphrey, 2014: A MapReduce technique to mosaic continental-scale weather radar data in real-time. IEEE J. *Select Topics in Applied Earth Obs. & Remote Sensing*, 7, 721-732.

Lakshmanan, V., T. Smith, K. Hondl, G. J. Stumpf, and A. Witt, 2006: A real-time, three-dimensional, rapidly updating, heterogeneous radar merger technique for reflectivity, velocity, and derived products. Wea. Forecasting, **21**, 802–823.

Lang, S., W. Tao, X. Zeng, and Y. Li, 2011: Reducing the biases in simulated radar reflectivities from a bulk microphysics scheme: Tropical convective systems. J. Atmos. Sci., 68, 2306–2320. doi: 10.1175/JAS-D-10-05000.1

Lawrence, M. B., L. A. Avila, J. L. Beven, J. L. Franklin, R. J. Pasch, and S. R. Stewart, 2005: Atlantic hurricane season of 2003. *Mon. Wea. Rev.*, **133,** 1744-1773.

MacEachren, A. M., 1985: Compactness of geographic shape: comparison and evaluation of measures. *Geografiska Annaler*, **67B,** 53-67.

Maddox, R. A., 1980: Mesoscale convective complexes. *Bull. Amer. Meteor. Soc.*, **61,** 1374 - 1387.

Matyas, C. J., 2007: Quantifying the shapes of US landfalling tropical cyclone rain shields. *The Professional Geographer*, **59,** 158-172.

Matyas, C. J., 2009: A spatial analysis of radar reflectivity regions within Hurricane Charley (2004). *J. Appl. Meteor. Clim.*, **48,** 130-142.

Matyas, C. J., 2010: Associations between the size of hurricane rain fields at landfall and their surrounding environments. *Meteor. and Atmos. Physics*, **106,** 135-148.

Matyas, C. J., and J. Tang, 2015: Measuring gaps in tropical cyclone rainbands using Level II radar reflectivity data. *69th Annual IHC meeting*, Jacksonville, FL.

NOAA, Service Assessment: Hurricane Isabel, September 18-19, 2003. [http://www.weather.gov/os/assessments/pdfs/isabel.pdf.]

Skamarock, W., J. Klemp, J. Dudhia, D. Gill, and D. Barker, 2008: *A description of the Advanced Research WRF version 3. NCAR Tech*. Note NCAR/TN-4751STR.

Steiniger, S. and E. Bocher 2009: An overview on current free and open source desktop GIS developments. Intl. J. of Geog. Info. Sci., **23**, 1345-1370.

Stoelinga, M. T., 2005: Simulated equivalent reflectivity factor as currently formulated in RIP: Description and possible improvements. *White Pap.*, **5**.

Tang, J. and C. J. Matyas, 2015: Fast playback framework for analysis of ground-based Doppler radar observations using map-reduce technology. *J. Oceanic and Atmos. Tech*., in revision.

Wang, W., D. Barker, J. Bray, C. Bruyere, M. Duda, J. Dudhia, D. Gill, and J. Michalakes, 2012: User's Guide for Advanced Research WRF (ARW) Modeling System Version 3.

Wang, Y., 2002: An explicit simulation of tropical cyclones with a triply nested movable mesh primitive equation model: TCM3. Part II: Model refinements and sensitivity to cloud microphysics parameterization. *Mon. Weather Rev.*, **130**, 3022–3036,

Warner, T. T., and H.-M. Hsu, 2000: Nested-Model Simulation of Moist Convection: The Impact of Coarse-Grid Parameterized Convection on Fine-Grid Resolved Convection. *Mon. Weather Rev.*, **128**, 2211–2231, doi:10.1175/1520-0493(2000)128<2211:NMSOMC>2.0.CO;2.

Williams, E. A., and E. A. Wentz, 2008: Pattern analysis based on type, orientation, size, and shape. *Geographical Analysis*, **40,** 97-122.

Zick, S. E., and C. J. Matyas, 2014: Moisture budgets in U.S. landfalling tropical cyclones and implications for rainfall. *ICMCS-X meeting*, Boulder, CO.